Applied Science and Innovative Research
ISSN 2474-4972 (Print) ISSN 2474-4980 (Online)
Vol. 9, No. 1, 2025
www.scholink.org/ojs/index.php/asir

Original Paper

Design and Analysis of Non-Contact Power Supply System for Wireless Monitoring Node of Ship's Water Lubricated Bearing

Chengfeng Li[1], Nan Wang[1*], Deyang Zhao[1], Huabin Jing[1], Jiayun Qi[1] & Mingjin Zhang[1]

[1] Shaanxi University of Technology, Hanzhong, Shaanxi 723000, China

[1] Chengfeng Li is the first author of this paper

[*] Nan Wang is the corresponding author of this paper

Received: December 21, 2024   Accepted: January 18, 2025   Online Published: January 25, 2025

doi:10.22158/asir.v9n1p64   URL: http://doi.org/10.22158/asir.v9n1p64

Abstract

The wireless sensor monitoring node for the online monitoring of various parameters of the ship's water-lubricated bearing rotates with the shaft during its operation. Therefore, how to ensure a continuous power supply to the node under the rotating working condition is an urgent problem to be solved. In this paper, a non-contact power supply method is adopted to design a magnetically coupled inductive non-contact power supply system, and experimental verification is carried out. Firstly, the non-contact power supply method is described, a node energy consumption model is established for the existing wireless monitoring nodes, and the energy consumption test is conducted. Then, a magnetically coupled inductive non-contact power supply system is designed, and the output of the system circuit is simulated and analyzed. Finally, the experimental test of the power supply system is carried out to study various factors that affect the performance of the power supply system. The research results show that the rotational speed is not the key factor affecting the power supply effect of the system, and the air gap of the coupling mechanism is the key factor affecting the power of the power supply system. The output power of the power supply system increases with the increase of the air gap, and the output efficiency decreases with the increase of the air gap. Considering the influence of the efficiency factor of the power supply system, the 5mm air gap is the optimal working air gap of the power supply system, and the system output power can reach 15.9 W at this time.

Keywords

Water-lubricated bearing, Wireless monitoring node, Magnetically coupled inductive non-contact power supply method

1. Introduction

Bearings are crucial components in the operation of ships. To ensure their stable and reliable operation, it is usually necessary to conduct online condition monitoring. The traditional condition monitoring technology for water-lubricated bearings is a wireless testing method powered by batteries (Wang Nan, Yang Litao, Liang Yingxuan, et al., 2019). This method uses a wireless point-to-point approach to monitor the operating parameters of the bearings. Although it is convenient for system design, it cannot achieve long-term online monitoring. It is necessary to stop the machine regularly to replace the batteries, which is very inconvenient and affects the overall operation of the ship. Shang Lixin et al. (2023) employed a set of wireless temperature monitoring nodes. By optimizing the software and hardware structure of the nodes to reduce power consumption, the power supply duration of the temperature monitoring nodes was extended. However, it is still limited by the battery-powered method. The self-powered method and the non-contact power supply method, due to their technical characteristics, can address the limitations of the battery-powered method and can meet the power supply requirements for the online monitoring of monitoring nodes (Li Jianpo, Li Shuo, Wang Yijun, et al., 2024; Yu Jichao, Zhou Zhiwei, & Sun Bo, 2023).

The self-powered method is to collect energy in the working environment of the device, such as thermal energy, wind energy, mechanical energy, etc. Qi Tianbo et al. (2021) proposed a rotational energy collection method for water-lubricated bearings, using a permanent magnet generator to collect the rotational energy of the rotating shaft to power the monitoring node. However, this scheme is overly affected by the rotational speed and the use of a permanent magnet generator requires reserving space at the stern of the ship during the ship design, lacking universality. Xue Enchi et al. (2022) employed micro or even nano-scale generators to convert pressure, friction, or thermal energy into electrical energy to power the wireless temperature monitoring device. However, the sensor needs to be embedded during the production process of the water-lubricated bearing, and the measuring point needs to be located at the easily worn area at the tail end of the shafting. The embedding cost of the sensor is high, and once it is damaged during operation, it is not easy to replace.

The non-contact power supply method realizes the energy transmission without electrical connection between the primary side and the secondary side through the electromagnetic coupling mechanism. Qi Junlin et al. (2024) applied the non-contact power supply technology to solve the power supply problem of the monitoring system of the floating mooring bollard of a large single-stage ship lock, achieving an energy transmission of 184.36 W with an efficiency of 67.3%. Wang Fangzhe et al. (2018) applied the non-contact power supply technology in the wireless temperature monitoring of the inner ring of the ball bearing, and solved the power supply problem of the monitoring node through the spatially nested coil, but did not further explore the factors affecting the power supply effect for research.

In conclusion, in this paper, the non-contact power supply method is adopted to solve the power supply problem of the wireless monitoring node of the water film pressure. A set of magnetic coupling inductive non-contact power supply system is designed, and the factors affecting the power supply effect of the system are studied.

2. Description of the Wireless Power Supply Method for Nodes

The schematic diagram of the wireless power supply method for the wireless monitoring node of the water-lubricated bearing is shown in Figure 1. This node is mainly used to monitor the water film pressure of the bearing. The water film pressure data is collected by the wireless monitoring node and wirelessly transmitted to the upper computer software for monitoring after signal processing. During the above process, the wireless monitoring node rotates with the shaft. To ensure the continuity and safety of the power supply process, a non-contact power supply method is adopted, which is described as follows: The DC power is provided by the regulated power supply and converted into AC power through the inverter circuit and then transmitted to the electromagnetic coupling mechanism. The primary side of the electromagnetic coupling mechanism is fixed on the test bench through the acrylic bracket, and the secondary side is fixed on the end cover of the wireless monitoring node. When the bearing rotates, the electrical energy is transmitted from the primary side to the node on the secondary side through the electromagnetic coupling of the coil. The electrical energy is transmitted from the static side of the primary side to the rotating side of the secondary side without electrical connection. The AC electricity induced by the secondary side is converted into DC electricity after rectification and filtering, and transmitted to the battery management circuit. The battery management circuit boosts the current and transmits it to the voltage and current stabilization circuit, and then it is delivered to the wireless monitoring node after voltage and current stabilization. When there is an external power supply input, the battery management circuit directly supplies power to the wireless monitoring node and charges the battery to ensure the battery power. When the external power supply input is lost, the two batteries supply power to the node to maintain the monitoring requirements. After troubleshooting the external power supply failure, the charging is resumed.

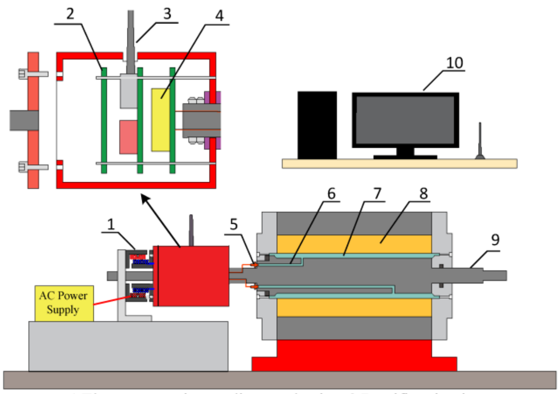

1.Electromagnetic coupling mechanism 2.Rectifier circuit
3.Wireless monitoring node 4.Battery management circuit
5.Water film pressure sensor 6.Influence hole 7.Water film
8.Water lubrication bearing 9.Spindle 10.Upper computer

Figure 1. Schematic Diagram of the Wireless Power Supply Method for Nodes

The principle of wireless power supply is shown in Figure 2, which mainly includes four parts: high-frequency inverter, electromagnetic coupling mechanism, rectifier filter, and load. The input of the system is direct current. The inverter is used to invert the direct current into high-frequency alternating current and then inject it into the primary side coil to generate a high-frequency alternating magnetic field. The secondary side coil generates alternating current with the same frequency through electromagnetic coupling of the alternating magnetic field, and then it is converted into direct current through the rectifier and supplies power to the load after being filtered by the inductor and capacitor. In this process, in order to reduce the reactive power loss of the system, it is also necessary to connect (or parallel) compensation capacitors Cp and Cs on both sides of the coupling mechanism to compensate for the leakage inductance of the coupling mechanism and improve the output power of the system.

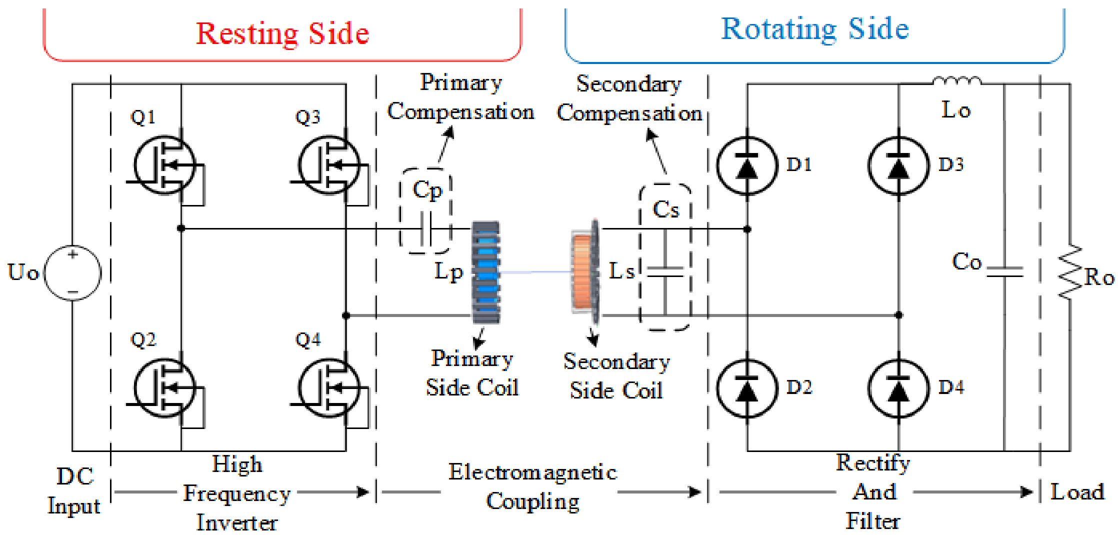

Figure 2. Wireless Power Supply Schematic Diagram

3. Composition and Energy Consumption Calculation of Wireless Monitoring Nodes

The structure of the wireless monitoring node for water film pressure is shown in Figure 3, including: sensor, constant current source, STM32 microcontroller, and wireless transceiver module. The sensor adopts the Dytran 2200v1 piezoelectric pressure sensor. The constant current source supplies power to the water film pressure sensor, and it also needs to be powered itself. The STM32 microcontroller is STM32F103ZET6. The wireless communication module uses DIGI Xbee3, which is responsible for implementing the communication protocol and sending the node data.

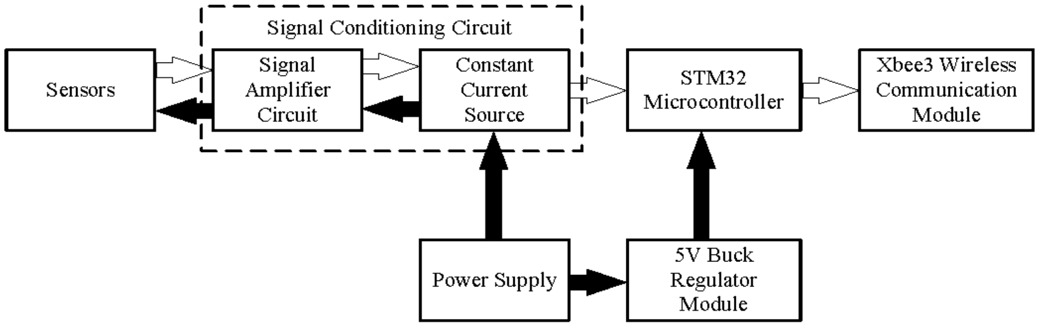

Figure 3. Structural Diagram of the Wireless Monitoring Node for Water Film Pressure

Due to the many factors that affect the energy consumption of the node, such as the modulation mode, data rate, transmission power, circuit module composition, and operation cycle adopted by the node, only an estimate of its energy consumption is made. Firstly, a multimeter is used to measure the hardware energy consumption of the wireless monitoring node. The energy consumption of the voltage reduction module is ignored. The energy consumption of the sensor and the signal conditioning circuit are in a series connection. For the convenience of the experimental test, only the constant current source is measured. The measurement results are shown in Table 1. The power consumption of the hardware circuit of the node circuit is 5.42 W.

Table 1. Node Energy Consumption

Circuit	Voltage V	Current A	Power W
Microcontroller	5	0.5	2.5
Constant Current Source	24	0.08	1.92
Xbee3	5	0.2	1

The energy consumption of the wireless monitoring node is not only related to itself but also greatly related to the amount of data transmitted. Therefore, a node energy consumption model as shown in the following figure is established (Kadhim, M. A. A., M. K. A. A., & Abdulhussein, S. A., 2023). Among them, E_{bit} is the energy consumption for the node to transmit one bit of data; ε is the energy parameter of the transmission amplifier; d is the interval between adjacent nodes for data transmission; E_{tx} and E_{rx} are the energies required for the node to transmit and receive K bits of data, respectively. The relevant parameters are shown in Table 2.

Table 2. Energy Consumption Model Parameters

Parameters	Value
ε	10 pJ/bit/m^2
E_{bit}	50 nJ/bit
d	5 m

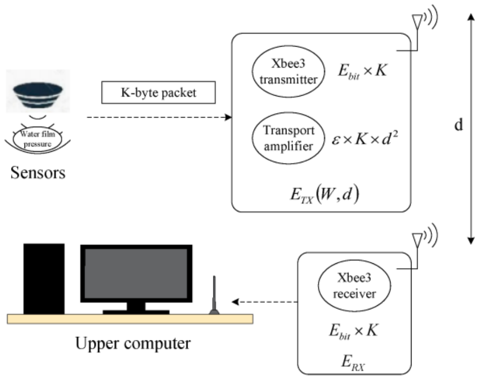

Figure 4. Energy Consumption Model of Wireless Nodes

$$E_{TX}(W,d) = E_{bit} \times K + \varepsilon \times K \times d^2 \quad (1)$$

$$E_{RX}(W) = E_{bit} \times K \quad (2)$$

This node has 5 channels. When K is 115200 bits and the communication baud rate is 115200 bit/s, the power consumed by the node to send data per second is approximately 0.005904 W, and the energy consumption for receiving data is approximately 0.00576 W.

In conclusion, the energy consumption of the wireless node under working conditions is approximately 5.42576 W.

4. Simulation and Design of Wireless Power Supply System

The wireless power supply device is shown in Figure 5, including an inverter circuit, a primary-side compensation topology, an electromagnetic coupling mechanism, a secondary-side compensation topology, a rectifier filter circuit, and a battery management circuit. The inverter circuit converts the current of the DC stabilized power supply into a high-frequency alternating current. After compensation, the current transmits the electrical energy to the secondary side (the electromagnetic coupling mechanism on the rotating side) on the rotating shaft through the primary side (the electromagnetic coupling mechanism on the stationary side). After rectification and filtering, it is converted into direct current and transmitted to the power management circuit. The power management circuit can directly supply power to the load. When there is an external power supply, it ensures that the battery power of both the first and second circuits is sufficient while supplying power. By default, the first circuit is used for power supply. This can meet the design requirements of online node monitoring. In the special case of a failure in the external power input, the two batteries can alternately and continuously supply power, and the online monitoring can continue after the power supply hazard is eliminated.

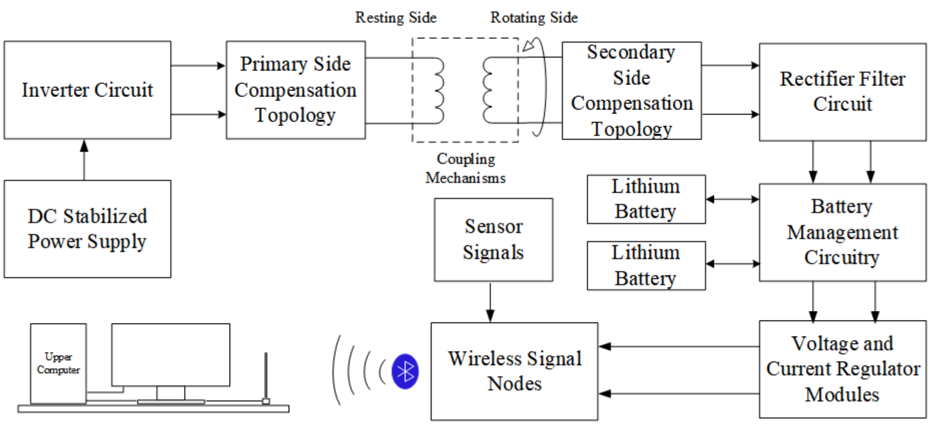

Figure 5. Composition of Wireless Power Supply System

Firstly, a simulation circuit of the inverter circuit, coupling coil, and rectifier filter circuit is established as shown in Figure 6. A simulation analysis and comparison of the output effects before and after using the LC circuit for filtering are carried out. The simulation circuit starts from a constant voltage source. Under a 14V DC input, two complementary PWM waves with a dead zone are formed by V2 to V5 to control the four MOS transistors M1 to M4, converting the DC power into AC power. After passing through the primary-side compensation topology C21 and the coupling coil, and then the secondary-side compensation topology C22, it is converted into DC power through the full-bridge uncontrolled rectifier circuit composed of D1 to D4. After being filtered by the LC circuit, it is output to the resistive load.

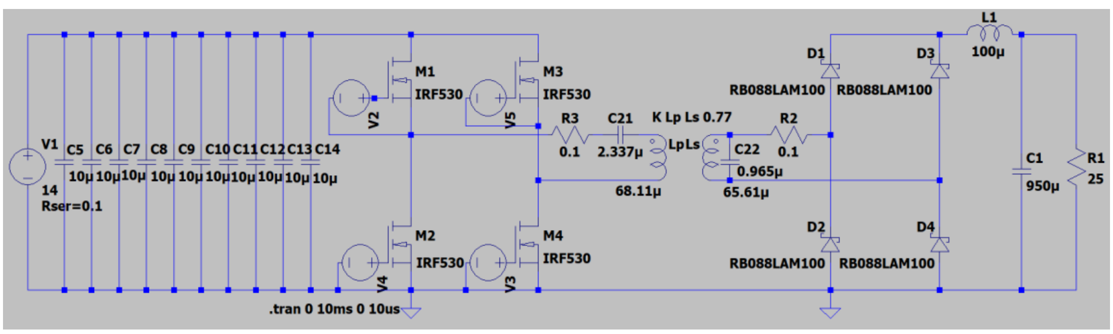

Figure 6. Schematic Diagram of Wireless Power Supply System

The schematic diagram of the charging management circuit is shown in Figure 7, and it can be mainly divided into three modules: the lithium battery charging circuit, the single-chip microcomputer acquisition and control circuit, and the output switching circuit. The lithium battery charging circuit uses the PW4203 chip, with a charging voltage of DC 4.5V to 23V and a charging current of 0 to 2A. Two 7.4V rechargeable lithium battery packs are connected in parallel to the output line for electrical energy storage. When there is an external power supply, the single-chip microcomputer and ADC chip are used to monitor the battery voltage. The two-channel PWM signals EN1 and EN2 are used to control the two chips and the MOS transistor switch to output the current. After the current is boosted by the SC3671 chip, a final output voltage of 24V is obtained. The circuit can directly supply power to the load. When the battery of one channel is insufficient, it is switched to the output of the battery of the second channel. When the battery of the second channel is outputting, the battery of the first channel is charged, and the same principle applies to the second channel in a cyclic manner. When there is an external power supply, it ensures that the battery power of both the first and second channels is sufficient. In the special case of losing the external power supply input, the two sets of batteries can alternately supply power through the two channels, enabling continuous power supply during the power supply replacement and maintenance process, meeting the design requirements of online node monitoring.

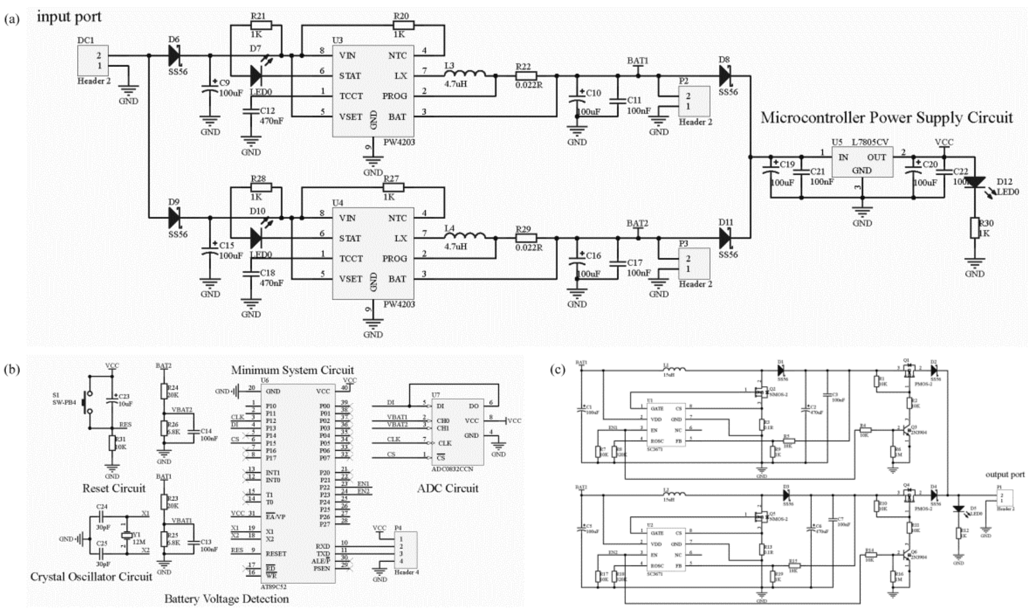

Figure 7. Battery Management Circuit (a) Battery Charging Circuit, (b) Battery Voltage Monitoring and Control Circuit, (c) Battery Voltage Monitoring and Control Circuit

The simulation results are shown in Figure 8. After using the LC circuit for filtering, the voltage and current ripples on the load resistor are significantly reduced. The reason is that the inductor L filters out the high-frequency part of the output current of the rectifier circuit, and the capacitor C can reduce the ripple magnitude of the output current of the rectifier circuit through its own charging and discharging. Therefore, an LC filter circuit needs to be added in the circuit design.

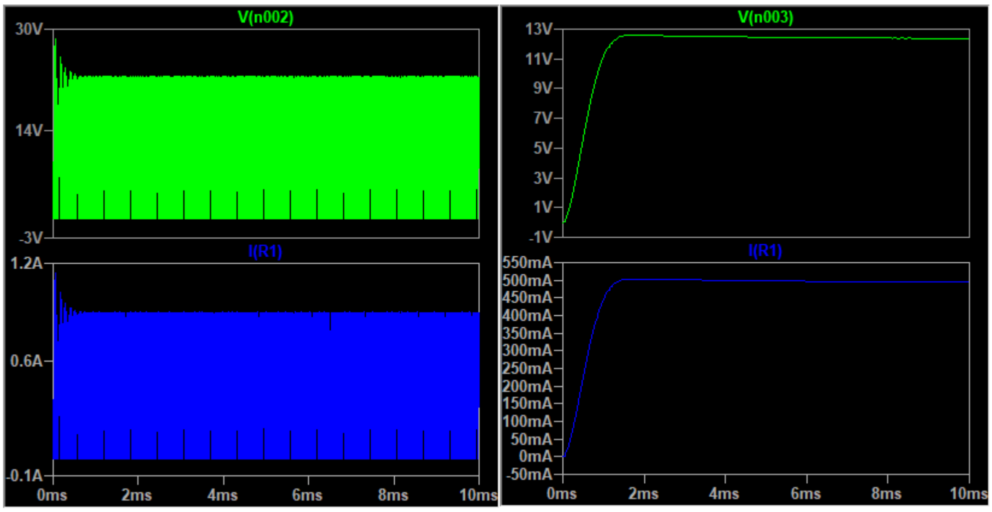

(a) Before Adding L-C Circuit Filtering (b) After Adding L-C Circuit Filtering

Figure 8. Simulation Output Waveforms of Wireless Power Supply System

4. Laboratory Test

The non-contact power supply experimental scheme for the water-lubricated bearing monitoring node is shown in Figure 9. A direct current is provided by a DC stabilized power supply and is inverted into a high-frequency alternating current through an inverter circuit. After primary-side compensation, it is input into the primary-side coil of the electromagnetic coupling mechanism. The secondary side induces an alternating current of the same frequency. After secondary-side compensation, it is rectified and filtered into a direct current to power the node through the battery management circuit, and also to charge the battery. The power management circuit ensures that the two sets of batteries are fully charged, and the output current supplies power to the wireless monitoring node. During this process, since the node and the secondary-side circuit rotate with the shaft, it is necessary to test the voltage at the measuring point through a brush, collect the current with a multimeter, and then use an oscilloscope (TDS3054C) to display the voltage test results.

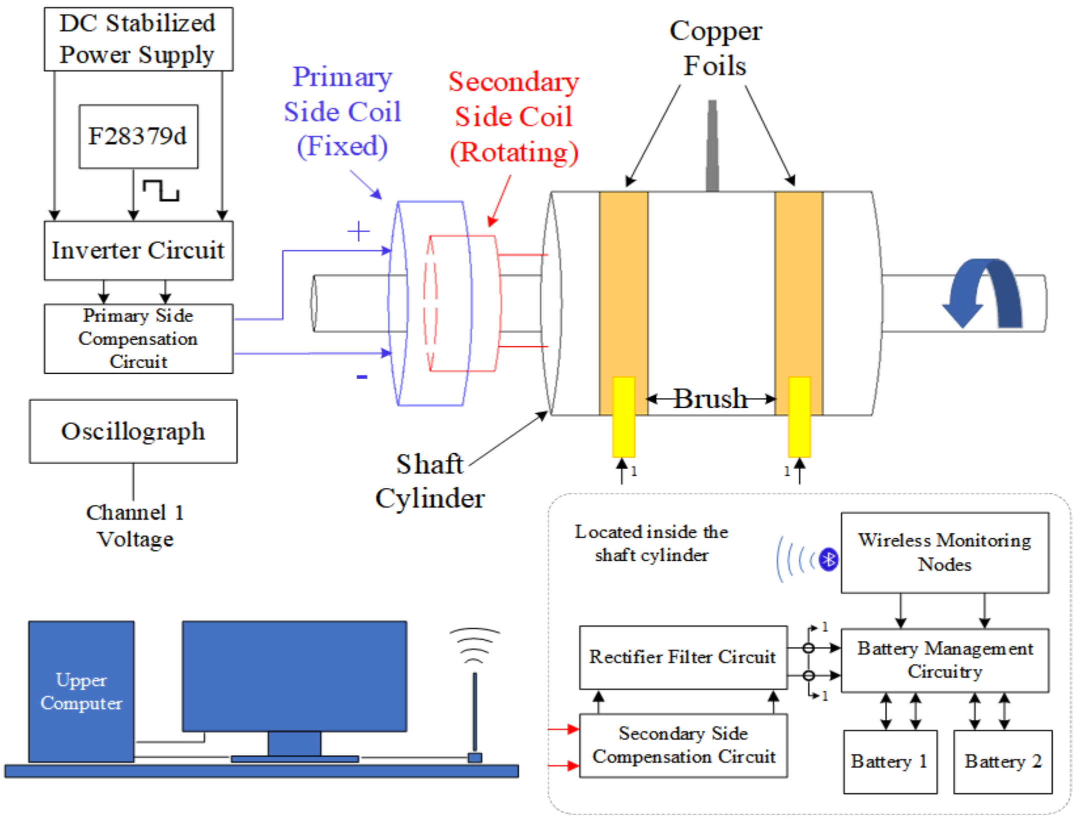

Figure 9. Schematic Diagram of Experimental Scheme for Non-contact Power Supply of Nodes

Table 3 shows the parameters of the power supply system used in the experimental test, and the experimental site is shown in Figure 10. Firstly, the stability of the power supply system was experimentally tested when the motor speed was 50 rpm and the air gap of the coupling mechanism was 5 mm. The input voltage of the battery management circuit is shown in Figure 13.

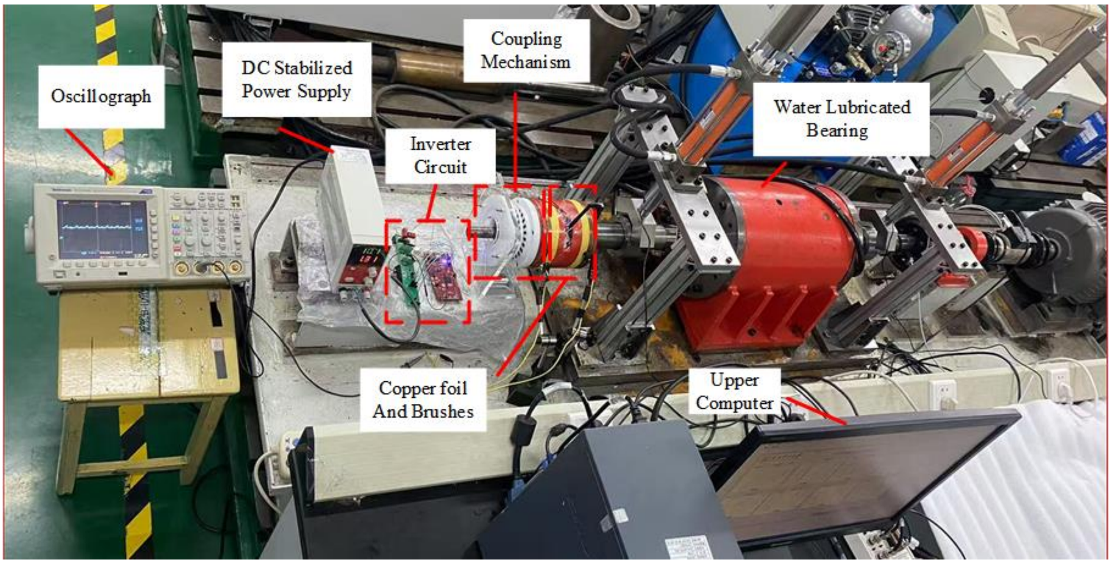

Figure 10. Test Site

Table 3. Test Parameter

Parameters	Value	Parameters	Value
U_{in}	14V	f	20kHz
L_p	68.11uH	L_s	65.61uH
C_p	2.337uF	C_s	0.965uF
M	51.87uH	C_1	951.71uF

As can be seen from Figure 11, the high and low levels of the output voltage of the power supply system after LC filtering can be stabilized at 9.3V. Further processing and amplification of the collected data reveal that there is still a ripple of up to 500 mA in the output voltage of the power supply system. The reason for this is that there are differences between the physical objects and the ideal circuit components, and the hardware circuit design has not been optimized. The output ripple of the system can still be optimized and reduced to improve the efficiency of the power supply system.

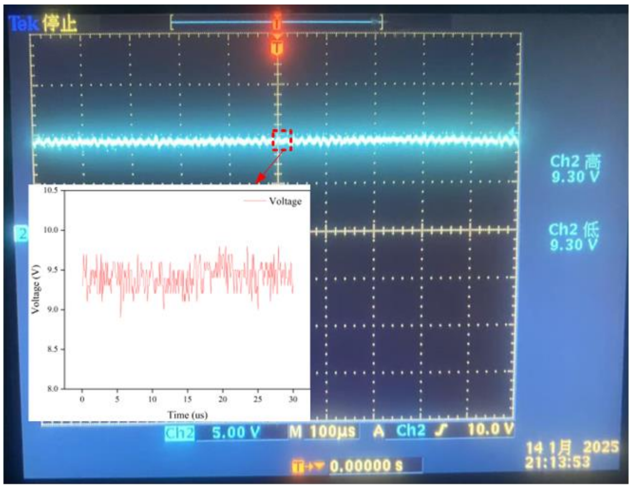

Figure 11. Output Voltage Waveform of Power Supply System with 5 mm Air Gap and 50 rpm

To further explore the factors affecting the power supply system, considering that the test bench operates under rotating conditions and a load needs to be applied during the operation. Since the monitoring node is located on the overhung side of the rotating shaft, the eccentricity of the rotating shaft will have an impact on the power supply effect of the power supply system. Therefore, the experiment needs to further conduct experimental tests on the power supply system output under different rotational speeds and air gaps. Figure 14 shows the system output voltage of the power supply system at a rotational speed of 0 - 400 rpm. Observing the voltage values of the system output in the figure, they are all around 9.39 V, indicating that the rotational speed is not the main factor affecting the power supply effect of the system.

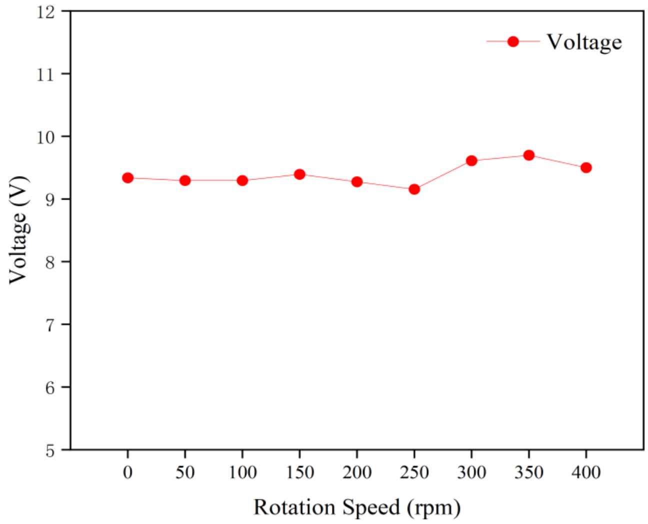

Figure 12. Output Voltage of Power Supply System under 0 - 400 rpm Rotational Speed

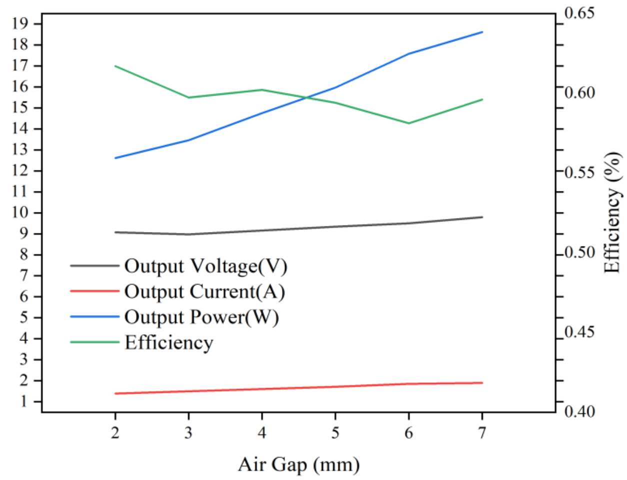

Figure 13. Output Power of Power Supply System with 2 - 7 mm Air Gap of Coupling Mechanism

As shown in Figure 15, the output power and system efficiency of the power supply system's coupling mechanism with an air gap ranging from 2mm to 7mm are presented. Observing the data in the figure, it can be seen that the minimum power of the system is 12.6 W. The output power of the power supply system increases with the increase of the air gap, reaching 18.6 W at a 7mm air gap, which can meet the energy consumption requirement of 5.4 W for the wireless monitoring node. However, the power supply efficiency of the power supply system decreases with the increase of the air gap. Considering the influence of the power supply system efficiency factor, 5mm air gap is the optimal working air gap for the power supply system.

5. Conclusion

To address the power supply problem of the online monitoring method for the operating status of water-lubricated bearings under rotating conditions, a non-contact power supply method is proposed and a non-contact power supply system is designed. Through a combination of establishing an energy consumption model of the monitoring node, circuit simulation, and experimental testing, the power supply effect of the non-contact power supply system is verified, and the factors affecting the power supply effect of the system are studied. The conclusions are as follows:

(1) The rotational speed is not the key factor affecting the power supply effect of the system, while the air gap of the coupling mechanism is the key factor affecting the system power supply.

(2) The air gap is proportional to the system output power and inversely proportional to the system output efficiency. Moreover, an air gap of 5 mm can balance the output power and output efficiency, making it the optimal operating air gap for the system. The minimum output power of the power supply system is 12.6 W, the maximum output power is 18.6 W, and the average output power can reach 15.49 W, which can meet the power supply requirements of the monitoring node.

(3) The subsequent research focus lies in further optimizing the compensation topology and the hardware circuit design to improve the transmission efficiency of the non-contact power supply system and the stability of the system output, so as to be applicable to more application scenarios under rotating conditions.

References

Kadhim, M. A. A., M. K. A. A., & Abdulhussein, S. A. Optimizing energy consumption in WSN-based IoT using unequal clustering and sleep scheduling methods. *Internet of Things*, 2023, 22.

Li Jianpo, Li Shuo, Wang Yijun, et al. Research Review on Magnetically Coupled Resonant Wireless Power Transfer Technology. *Electrical Measurement & Instrumentation*, 2024, *61*(08), 1-11.

Qi Juntao, Qin Tao, & Jiang Tao. Design of Floating Wireless Power Supply System for Floating Mooring Bollard of Ship Lock. *Port & Waterway Engineering*, 2024, (09), 173-179.

Qi Tianbo, Wang Nan, & Yang Litao. Research on the Power Supply Method for the Wireless Monitoring Node of the Water Film Pressure of the Water-Lubricated Bearing. *China Measurement & Test*, 2021, *47*(02), 13-18.

Shang Lixin, Jiao Xinquan, Chen Jianjun. Low-Power Optimization Design of Thermocouple Wireless Sensor Nodes. *Computer Measurement & Control*, 2023, *31*(01), 294-300.

Wang Fangzhe, Zhu Yongsheng, Yan Ke, et al. Wireless Monitoring Technology for Inner Ring Temperature of Rolling Bearing. *Journal of Mechanical Engineering*, 2018, *54*(22), 8-14.

Wang Nan, Yang Litao, Liang Yingxuan, et al. Non-contact Electromagnetic Loading Water-lubricated Bearing Monitoring System. *China Mechanical Engineering*, 2019, *30*(24), 3004-3009.

Xue Enchi, Guo Zhiwei, & Yuan Chengqing. Design and Performance Verification of Marine Intelligent Water-Lubricated Stern Bearing with Temperature Sensing. *China Mechanical Engineering*, 2022, *33*(14), 1639-1645.

Yu Jichao, Zhou Zhiwei, & Sun Bo. Research on Wireless Sensing Technology in Self-Powered Monitoring System for Coal Mine Machinery. *Coal Technology*, 2023, *42*(04), 202-204.